

## Cyclic Vinylogous TTF: a Potential Molecular Clip Triggered by Electron Transfer

Michel Guerro,<sup>†</sup> Roger Carlier,<sup>†</sup> Kamal Boubekeur,<sup>‡</sup> Dominique Lorcy,<sup>\*,†</sup> and Philippe Hapiot<sup>\*,†</sup>

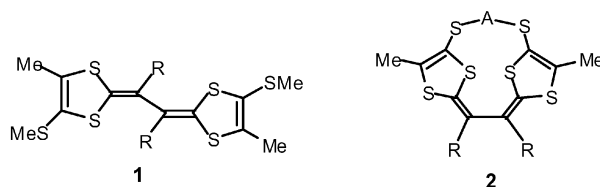
Contribution from the Synthèse et Electrolyse Organiques, UMR CNRS 6510, Université de Rennes 1, Campus de Beaulieu, 35042 Rennes Cedex, France, and Laboratoire de Sciences Moléculaires aux Interfaces, FRE CNRS 2068, Institut des Matériaux Jean Rouxel, 2 rue de la Houssinière, 44322 Nantes Cedex 3, France

Received October 11, 2002; E-mail: dominique.lorcy@univ-rennes1.fr; philippe.hapiot@univ-rennes1.fr

**Abstract:** Cyclic vinylogous tetrathiafulvalenes (TTFs) where the two dithiole rings are linked through the outer sulfur atoms with an alkyl chain of various lengths were synthesized by oxidative intramolecular coupling of bis(dithiafulvenes). Upon oxidation, these systems exhibit large molecular movements associated with electron transfers. Their electrochemical behaviors were investigated together with the X-ray crystallographic structures of several derivatives and compared with molecular geometry calculations. Dependent on the length of the alkyl chain, either a stretch or a clip movement can be observed. These conformational modifications were found to be fast and fully reversible and required only low oxidation potentials. The movements seem to be almost insensitive to the nature of the substituents or its steric hindrance on the central conjugated spacer.

### Introduction

Molecules where molecular movements can be triggered by simple electron transfer have become the focus of much attention for the design of molecular devices (switches, motors, sensors, etc.).<sup>1</sup> The control of the extent and nature of the conformational changes remains one of the principal challenges to achieve this goal. Within this frame, vinylogous tetrathiafulvalenes (TTFs) **1** prepared by oxidative coupling of 1,4-dithiafulvenes have recently attracted considerable attention due to the ability of this method for introducing various substituents (R) on the central conjugation.<sup>2–6</sup> The presence of the bulky substituents



R does not modify the donor ability of the molecules but prevents the donor to be planar due to steric interactions, inducing large molecular movements associated with the electron transfer.<sup>3a,4,7</sup> Dependent on the steric hindrance and the donating (or withdrawing) character of R, the oxidation of the TTF occurs either through a reversible bielectronic transfer leading directly to the dicationic state or through two reversible mono-electronic transfers corresponding to the consecutive formations of the radical cation and of the dication. The first observed experimental situation, named “potentials inversion”,<sup>8–10</sup> is a direct consequence of important structural changes in the TTF core<sup>11</sup>

<sup>†</sup> Université de Rennes 1.

<sup>‡</sup> Institut des Matériaux Jean Rouxel.

\* Corresponding authors phone: +33 2 23 23 59 39, Fax: +33 2 23 23 67 32. Email: dominique.lorcy@univ-rennes1.fr and philippe.hapiot@univ-rennes1.fr

- (1) For examples and general reviews about molecular devices triggered by electron transfers and related concepts, see for example (references therein): (a) Pease, A. R.; Jeppesen, J. O.; Stoddart, J. F.; Luo, Y.; Collier, C. P.; Heath, J. R. *Acc. Chem. Res.* **2001**, *34*, 433. (b) Collin J.-P.; Dietrich-Buchecker, C.; Gaviña, P.; Jimenez-Molero, M. C.; Sauvage, J.-P. *Acc. Chem. Res.* **2001**, *34*, 477. (c) Amendola, V.; Fabbri, L.; Mangano, C.; Pallavicini, P. *Acc. Chem. Res.* **2001**, *34*, 488.
- (2) (a) Kirmse, W.; Horner, L. *Liebigs Ann. Chem.* **1958**, *614*, 4. (b) Mayer, K.; Kröber, H. *J. Prakt. Chem.* **1974**, *316*, 907. (c) Cava, M. P.; Lakshmikantham, M. V. *J. Heterocycl. Chem.* **1980**, *17*, S39. (d) Schöberl, U.; Salbeck, J.; Daub, J. *Adv. Mater.* **1992**, *4*, 41. (e) Benahmed-Gasmi, A.; Frère, P.; Roncali, J.; Elandaloussi, E.; Orduna, J.; Garin, J.; Jubault, M.; Gorgues, A. *Tetrahedron Lett.* **1995**, *36*, 2983.
- (3) (a) Lorcy, D.; Carlier, R.; Robert, A.; Tallec, A.; Le Maguerès, P.; Ouahab, L. *J. Org. Chem.* **1995**, *60*, 2443. (b) Hapiot, P.; Lorcy, D.; Carlier, R.; Tallec, A.; Robert, A. *J. Phys. Chem.* **1996**, *100*, 14823. (d) Bellec, N.; Lorcy, D.; Robert, A.; Carlier, R.; Tallec, A. *J. Electroanal. Chem.* **1999**, *462*, 137.
- (4) (a) Ohta, A.; Yamashita, Y. *J. Chem. Soc., Chem. Commun.* **1995**, 1761. (b) Moore, A. J.; Bryce, M. R.; Skabara, P. J.; Batsanov, A. S.; Goldenberg, L. M.; Howard, J. A. K. *J. Chem. Soc., Perkin Trans. 1* **1997**, 3443. (c) Yamashita, Y.; Tomura, M.; Braduz Zaman, M.; Imaeda, K. *J. Chem. Soc., Chem. Commun.* **1998**, 1657.

- (5) (a) Fourmigué, M.; Johannsen, I.; Boubekeur, K.; Nelson C.; Batail, P. *J. Am. Chem. Soc.* **1993**, *115*, 3752. (b) Frère, P.; Benahmed-Gasmi, A. S.; Roncali, J.; Jubault, M.; Gorgues, A. *J. Chim. Phys.* **1995**, *92*, 863. (c) Gonzalez, S.; Martin, N.; Sanchez, L.; Segura, J. L.; Seoane, C.; Fonseca, I.; Cano, F. H.; Sedo, J.; Vidal-Gancedo, J.; Rovira, C. *J. Org. Chem.* **1999**, *64*, 3498. (d) Roncali, J. *J. Mater. Chem.* **1997**, *7*, 2307. (e) Lorcy, D.; Guerin, D.; Boubekeur, K.; Carlier, R.; Hascoat, P.; Tallec, A.; Robert, A. *J. Chem. Soc., Perkin Trans. 1* **2000**, 2719.
- (6) Hascoat, P.; Lorcy, D.; Robert, A.; Carlier, R.; Tallec, A.; Boubekeur, K.; Batail, P. *J. Org. Chem.* **1997**, *62*, 6086.
- (7) Hopf, H.; Kreutzer, M.; Jones, P. G. *Angew. Chem., Int. Ed.* **1991**, *30*, 1127.
- (8) (a) By opposition with the normal ordering of potentials where it is generally more difficult to remove a second electron than the first one.<sup>8b,c</sup> (b) Evans, D. H.; O'Connell, K. M. *Conformational Change and Isomerization Associated with Electrode Reactions in Electroanalytical Chemistry*; Bard, A. J., Ed.; Marcel Dekker: New York, 1986; Vol. 14, pp 113–207. (c) Evans, D. H.; Lehmann, M. W. *Acta Chem. Scand.* **1999**, *53*, 765.
- (9) Evans, D. H.; Hu, K. *J. Chem. Soc., Faraday Trans.* **1996**, *92*, 3983.

concerted with the electron transfers.<sup>9,12</sup> The induced conformational changes depend on the energetic stabilities of all the redox states that are related to the steric hindrance and electronic properties of the chemical groups present in the molecule.<sup>12</sup> In this connection, we have recently demonstrated that, through the choice of the substituent (R), it is possible to control in a large extent the relative stabilities of the different redox species.<sup>11,12</sup> As the motor of the molecular movement is the vinylogous TTF core itself, it seems therefore possible to adjust the amplitude of the movements by introducing different sources of steric strain without suppressing the donating ability. For instance, a link of various lengths connecting the two dithiole rings through the outer sulfur atoms may provide another way to control the extension and the nature of the movements associated with the electron transfer.<sup>13</sup> Besides the fundamental aspect of the investigations, vinylogous TTFs present the other advantages that are required in the design of molecular devices: high chemical stabilities for all the redox states, fast kinetics (both for the electron transfer and conformational changes), and fairly easy synthesis procedures. In this work, various cyclic vinylogous TTFs have been synthesized and the mechanism of their formation determined. Electrochemical methods were used for investigating the conformational changes, as their effects are detected through the thermodynamic and kinetics parameters of the electron transfers.<sup>8b-c,9,12,14</sup> The electrochemical behaviors were investigated together with the X-ray crystallographic structures of several derivatives of type **2** as well as molecular geometry optimizations in order to rationalize the observed experiments and identify the new parameters that control the molecular movement.

## Experimental Section

**Chemicals.** All the vinylogous tetrathiafulvalenes (TTFs) have been prepared by oxidative intramolecular coupling of bis-(1,4-dithiafulvenes) in a one-pot procedure by a two-step electrochemical synthesis: first an oxidation of the monomer and then a reduction of the solution.<sup>6</sup>

Acetonitrile was Uvasol quality (Merck). Dichloromethane was Rectapur quality (Prolabo). The supporting electrolytes  $\text{NEt}_4\text{BF}_4$  and  $\text{NBu}_4\text{BF}_4$  were from Fluka (puriss quality). Solutions were prepared freshly before experiments, and oxygen was removed by bubbling argon.

**Electrochemical Experiments.** All the cyclic voltammetry experiments were carried out at  $20 \pm 0.1$  °C using a cell equipped with a jacket allowing circulation of water from the thermostat. The working electrode was a 1 mm diameter either platinum or gold disk. It was carefully polished before each set of voltammograms with 1  $\mu\text{m}$  diamond paste and ultrasonically rinsed in absolute ethanol. Electrochemical instrumentation

consisted of a Tacussel GSTP4 programmer and of a home-built potentiostat equipped with a positive feedback compensation device.<sup>15</sup> The data were acquired with a 310 Nicolet oscilloscope. The counter electrode was a Pt wire, and the reference electrode, an aqueous saturated calomel electrode with a salt bridge containing the supporting electrolyte. The SCE electrode was checked against the ferrocene/ferricinium couple (considering the following  $E^\circ$  values  $E^\circ = +0.405$  V/SCE in acetonitrile and  $+0.528$  V/SCE in dichloromethane) before and after each experiment. Based on repetitive measurements, absolute errors on potentials were found to be around  $\pm 5$  mV. In situations of inverted potentials,  $\Delta E_p$  measurements (which do not require the standardization of the reference electrode) were repeated at least 10 times and averaged. Errors were found to be  $\pm 1$  mV.

Spectroelectrochemical measurements were performed with a platinum anode inserted in a modified 0.1 cm quartz cell according to a previously published procedure.<sup>16</sup>

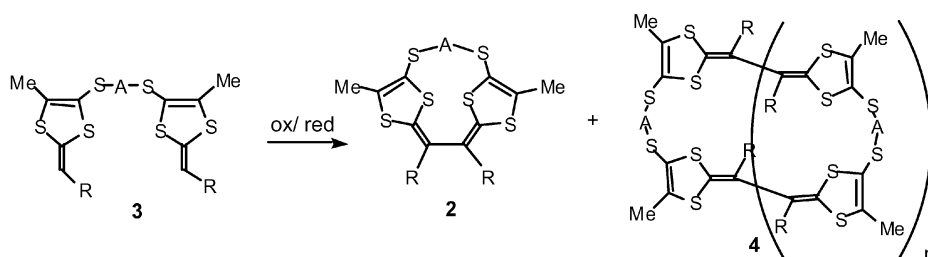
Numerical simulations of the voltammograms were performed with the commercial BAS Digisim Simulator 3.1<sup>17</sup> using the default numerical options with the assumption of planar diffusion. Butler–Volmer law was considered for the electron-transfer kinetics transfer. The transfer coefficient,  $\alpha$ , was taken as 0.5, and the diffusion coefficients were equal for all the species ( $D = 10^{-5}$  cm<sup>2</sup> s<sup>-1</sup>).

**Theoretical Modeling.** The calculations were performed using the Gaussian 98 package<sup>18</sup> for density functional and solvation calculations. Gas-phase geometries and electronic energies were calculated by full optimization without imposed symmetry of the conformations using the B3LYP<sup>19</sup> density functional with the 6-31G\* basis set,<sup>20,21</sup> starting from preliminary optimizations performed with semiempirical methods. Because of the difficulty to run frequency calculations with the large investigated molecules, the quality of the obtained minima was checked by restarting the optimizations from other conformations which led to the same optimized geometries. We checked that the spin contamination remains low ( $s^2 < 0.755$ ) for all the open shell B3LYP calculations. Solvation free energies were calculated on the gas-phase optimized conformations according to the SCRf (self-consistent reaction field) method using the IPCM method<sup>22</sup> and the B3LYP density functional. In this method, the solvent is treated as a continuum

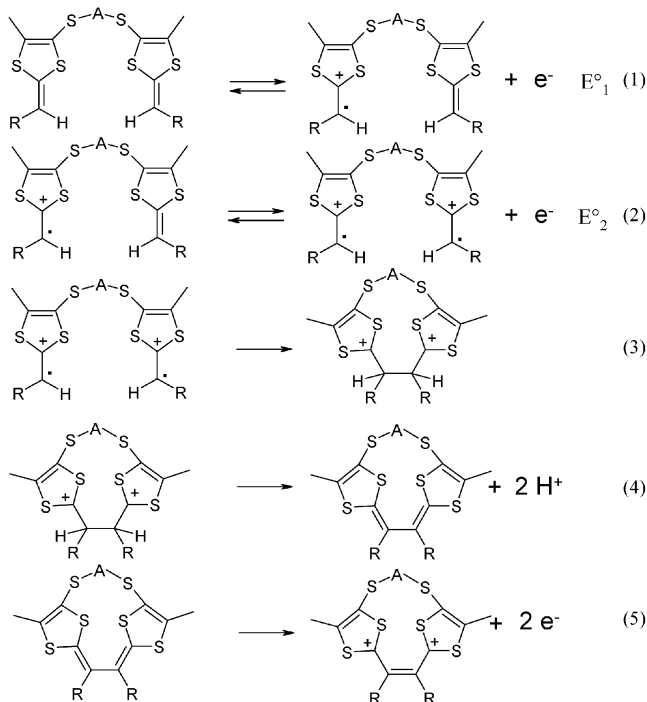
- (10) (a) Hu, K.; Evans, D. H. *J. Phys. Chem.* **1996**, *100*, 3030. (b) Hu, K.; Evans, D. H. *J. Electroanal. Chem.* **1997**, *423*, 29. (c) Speiser, B.; Würde, M.; Maichle-Mössmer, C. *Chem.—Eur. J.* **1998**, *4*, 222. (d) Dümmling, S.; Speiser, B.; Kuhn, N.; Weyers, G. *Acta Chem. Scand.* **1999**, *53*, 876.
- (11) (a) Lorcy, D.; Le Maguerès, P.; Rimbaud, C.; Ouahab, L.; Delhaes, P.; Carlier, R.; Tallec, A.; Robert, A. *Synth. Met.* **1997**, *86*, 1831. (b) Rimbaud, C.; Le Maguerès, P.; Ouahab, L.; Lorcy, D.; Robert, A. *Acta Crystallogr.* **1998**, *C54*, 679. (c) Yamashita, Y.; Tomura, M.; Imaeda, K. *Tetrahedron Lett.* **2001**, *42*, 4191.
- (12) Bellec, N.; Boubekour, K.; Carlier, R.; Hapiot, P.; Lorcy, D.; Tallec, A. *J. Phys. Chem. A* **2000**, *104*, 9750.
- (13) For example, see: Godbert, N.; Batsanov, A. S.; Bryce, M. R.; Howard, J. A. K. *J. Org. Chem.* **2001**, *66*, 713.
- (14) (a) Rathore, R.; Le Maguerès, P.; Lindeman, S. V.; Kochi, J. K. *Angew. Chem., Int. Ed.* **2000**, *39*, 809. (b) Heinze, J.; Willmann, C.; Bäuerle, P. *Angew. Chem., Int. Ed.* **2001**, *40*, 2861.

- (15) Garreau, D.; Savéant, J.-M. *J. Electroanal. Chem.* **1972**, *35*, 309.
- (16) Lexa, D.; Savéant, J.-M.; Ziegler, J. *J. Am. Chem. Soc.* **1977**, *99*, 2786.
- (17) Rudolph, M.; Reddy, D. P.; Felberg, S. W. *Anal. Chem.* **1994**, *66*, 589A.
- (18) Frisch, M. J.; Trucks, G. W.; Schlegel, H. B.; Scuseria, G. E.; Robb, M. A.; Cheeseman, J. R.; Zakrzewski, V. G.; Montgomery, J. A.; Stratmann, R. E.; Burant, J. C.; Dapprich, S.; Millam, J. M.; Daniels, A. D.; Kudin, K. N.; Strain, M. C.; Farkas, O.; Tomasi, J.; Barone, V.; Cossi, M.; Cammi, R.; Mennucci, B.; Pomelli, C.; Adamo, C.; Clifford, S.; Ochterski, J.; Petersson, G. A.; Ayala, P. Y.; Cui, Q.; Morokuma, K.; Malick, D. K.; Rabuck, A. D.; Raghavachari, K.; Foresman, J. B.; Cioslowski, J.; Ortiz, J. V.; Stefanov, B. B.; Liu, G.; Liashenko, A.; Piskorz, P.; Komaromi, I.; Gomperts, R.; Martin, R. L.; Fox, D. J.; Keith, T.; Al-Laham, M. A.; Peng, C. Y.; Nanayakkara, A.; Gonzalez, C.; Challacombe, M.; Gill, P. M. W.; Johnson, B. G.; Chen, W.; Wong, M. W.; Andres, J. L.; Head-Gordon, M.; Replogle, E. S.; Pople, J. A. *Gaussian 98*, revision A.9; Gaussian, Inc.: Pittsburgh, PA, 1998.
- (19) Becke, A. D. *J. Chem. Phys.* **1993**, *98*, 5648.
- (20) Hariharan, P. C.; Pople, J. A. *Chem. Phys. Lett.* **1972**, *16*, 217.
- (21) (a) Hybrid density functional methods with the 6-31G\* base have been used previously for calculations on neutral and radical cations of heterocycles containing sulphur atoms and on extended TTF and found to give a good qualitative description of properties. For example, see ref 21b,c. (b) Hernández, V.; Mugaruma, H.; Hotta, S.; Casado, J.; López Navarrete, J. T. *J. Phys. Chem. A* **2000**, *104*, 735. (c) Keszthelyi, T.; Grage, M. M.-L.; Offersgaard, J. F.; Wilbrandt, R.; Svendsen, C.; Mortensen, O. S.; Pedersen, J. K.; Jensen, H. J. A. *J. Phys. Chem. A* **2000**, *104*, 2808.

## Scheme 1



## Scheme 2



of a uniform dielectric constant in which the solute is placed into a cavity defined as an isodensity surface of the molecules. The value for the isodensity surface was chosen as 0.001 electrons/bohr<sup>3</sup> as used in previous published calculations.

## Results and Discussion

**Oxidation of Bis(1,4-dithiafulvenes).** A series of cyclic vinylogous tetrathiafulvalenes **2** were prepared by oxidation of the corresponding bis(1,4-dithiafulvenes) **3** (Scheme 1). These precursors were prepared according to a previously published procedure from the mesoionic dithiole.<sup>6,23</sup> The versatility of this synthetic strategy allows us to vary in a large extent both the length of the alkyl chain *A* between the two dithiole cores and the substituent *R*. The first variation in the molecular structure of **3** was to change the length of the alkyl chain (*A* = (CH<sub>2</sub>)<sub>*n*</sub> with *n* = 12, 4, 3) as a way to control or restrain the amplitude of the molecular movement with the redox state in **2**. For each chain length, we modify the position and the nature (donating or withdrawing) of the substituents present on the phenyl group (see Table 1).

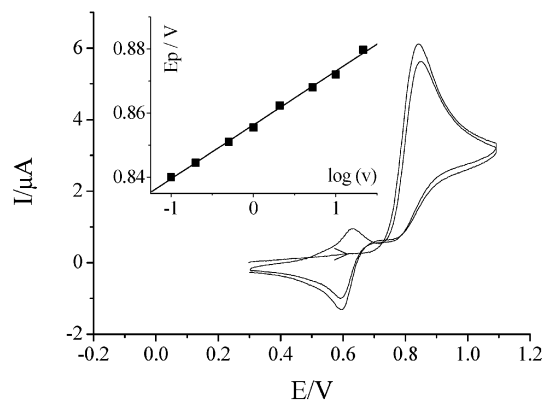


**Figure 1.** Repetitive cyclic voltammetry of 1,4-dithiafulvenes **3** (*A* = (CH<sub>2</sub>)<sub>4</sub>, *R* = *o*-NCC<sub>6</sub>H<sub>4</sub>) oxidation on a 1 mm diameter disk gold electrode in acetonitrile + 0.1 mol L<sup>-1</sup> NBu<sub>4</sub>BF<sub>4</sub>. Scan Rate 0.1 V s<sup>-1</sup>. Insert: variation of the peak potential with the scan rate ( $\log(v)$ ). Conc<sub>n</sub> = 10<sup>-3</sup> mol L<sup>-1</sup>. The symbol > shows the first scan. Reference electrode: SCE.

The cyclic vinylogous tetrathiafulvalenes **2** were then obtained by a macroscale oxidative cyclization of **3** in a one-pot procedure by a two-step electrochemical synthesis: first the oxidation of **3** and then a reduction of the produced dication. Workup of the solution shows that the major compound is the cyclic vinylogous tetrathiafulvalenes **2**, indicating that the 1,4-dithiafulvenes **3** undergo intramolecular coupling even when the bridging chain is short or when bulky substituents are located on the ortho position of the aromatic core. As other minor products, we have also isolated cyclic vinylogous tetrathiafulvalenes **4** resulting from intermolecular couplings (Scheme 1). To get better insights about the reactions involved in the electrochemical synthesis of **2**, we performed detailed electrochemical investigations by cyclic voltammetry on one of the compounds **3** (the cyclic voltammogram responses of the other 1,4-dithiafulvenes derivatives exhibit the same general patterns). A typical voltammogram of the oxidation of **3** in acetonitrile is presented in Figure 1. Examination of the oxidation peak for **3** in acetonitrile shows that it corresponds to the exchange of two electrons per molecule and that the peak potential *E<sub>p</sub>* varies linearly with the logarithm of the scan rate *v* with the slope ( $\partial E_p / \partial \log(v)$ ) = 16.8 mV for a 10-fold increase (between 0.1 and 20 V s<sup>-1</sup>) and is not sensitive to the value of the initial concentration *C* of **3** ( $\partial E_p / \partial \log(C)$ ) = 0 (between 3 × 10<sup>-5</sup> and 5 × 10<sup>-4</sup> mol L<sup>-1</sup>). After the oxidation peak was scanned, a new redox system appears on the reverse potential scan at a lower value, indicating the formation of the dimer. For the synthesis of the unlinked TTF **1**, we previously found that the oxidative dimerization of the 1,4-dithiafulvenes occurs through a radical cation–radical cation coupling mechanism.<sup>3b</sup> We may expect that the intramolecular coupling of **3** proceeds through a similar pathway, that is, a mechanism involving first the double oxidation of the bis-

(22) (a) Foresman, J. B.; Keith, T. A.; Wiberg, K. B.; Snoonian, J.; Frisch, M. J. *J. Phys. Chem.* **1996**, *100*, 16098. (b) For a general review about solvation methods, see: Cramer, J.; Truhlar, D. G. *Chem. Rev.* **1999**, *99*, 2161.

(23) (a) Boubekeur, K.; Lenoir, C.; Batail, P.; Carlier, R.; Tallec, A.; Le Paillard, M. P.; Lorcy, D.; Robert, A. *Angew. Chem., Int. Ed. Engl.* **1994**, *33*, 1379. (b) Hascoat, P.; Lorcy, D.; Robert, A.; Boubekeur, K.; Batail, P.; Carlier, R.; Tallec, A. *J. Chem. Soc., Chem. Commun.* **1995**, 1229.



**Table 1.** Oxidation Potentials vs SCE and  $\Delta E^\circ$  of Vinylogous TTF **1** and Cyclic Vinylogous TTF **2(n)** in  $\text{CH}_2\text{Cl}_2$ 

compound <sup>a</sup>	R	A	$E_{1/2}/V$ ( $\Delta E_p/mV$ )	$\Delta E^\circ/mV^b$
<b>1a</b>	<i>p</i> -NCC <sub>6</sub> H <sub>4</sub>		0.651 (35)	-25
<b>1b</b>	<i>o</i> -NCC <sub>6</sub> H <sub>4</sub>		0.551 (57), 0.767 (70) <sup>c</sup>	216
<b>1c</b>	C <sub>6</sub> H <sub>5</sub>		0.519 (104) <sup>c</sup>	76
<b>1d</b>	<i>p</i> -MeOC <sub>6</sub> H <sub>4</sub>		0.468 (143) <sup>c</sup>	104
<b>1e</b>	<i>o</i> -MeOC <sub>6</sub> H <sub>4</sub>		0.293 (59), 0.551 (63) <sup>c</sup>	258
<b>2a(12)</b>	<i>p</i> -NCC <sub>6</sub> H <sub>4</sub>	(CH <sub>2</sub> ) <sub>12</sub>	0.705 (57)	36
<b>2b(12)</b>	<i>o</i> -NCC <sub>6</sub> H <sub>4</sub>	(CH <sub>2</sub> ) <sub>12</sub>	0.624 (62), 0.800 (83) <sup>c</sup>	176
<b>2c(12)</b>	C <sub>6</sub> H <sub>5</sub>	(CH <sub>2</sub> ) <sub>12</sub>	0.556 (116) <sup>c</sup>	85
<b>2d(12)</b>	<i>p</i> -MeOC <sub>6</sub> H <sub>4</sub>	(CH <sub>2</sub> ) <sub>12</sub>	0.510 (150) <sup>c</sup>	110
<b>2e(12)</b>	<i>o</i> -MeOC <sub>6</sub> H <sub>4</sub>	(CH <sub>2</sub> ) <sub>12</sub>	0.341 (69), 0.616 (74) <sup>c</sup>	275
<b>2a(4)</b>	<i>p</i> -NCC <sub>6</sub> H <sub>4</sub>	(CH <sub>2</sub> ) <sub>4</sub>	0.717 (37)	-13
<b>2b(4)</b>	<i>o</i> -NCC <sub>6</sub> H <sub>4</sub>	(CH <sub>2</sub> ) <sub>4</sub>	0.731 (49)	24
<b>2c(4)</b>	C <sub>6</sub> H <sub>5</sub>	(CH <sub>2</sub> ) <sub>4</sub>	0.622 (35)	-25
<b>2d(4)</b>	<i>p</i> -MeOC <sub>6</sub> H <sub>4</sub>	(CH <sub>2</sub> ) <sub>4</sub>	0.571 (37)	-13
<b>2e(4)</b>	<i>o</i> -MeOC <sub>6</sub> H <sub>4</sub>	(CH <sub>2</sub> ) <sub>4</sub>	0.529 (44)	13
<b>2a(3)</b>	<i>p</i> -NCC <sub>6</sub> H <sub>4</sub>	(CH <sub>2</sub> ) <sub>3</sub>	0.736 (39)	-3
<b>2b(3)</b>	<i>o</i> -NCC <sub>6</sub> H <sub>4</sub>	(CH <sub>2</sub> ) <sub>3</sub>	0.759 (39)	-3
<b>2c(3)</b>	C <sub>6</sub> H <sub>5</sub>	(CH <sub>2</sub> ) <sub>3</sub>	0.641 (38)	-7
<b>2d(3)</b>	<i>p</i> -MeOC <sub>6</sub> H <sub>4</sub>	(CH <sub>2</sub> ) <sub>3</sub>	0.595 (37)	-13
<b>2e(3)</b>	<i>o</i> -MeOC <sub>6</sub> H <sub>4</sub>	(CH <sub>2</sub> ) <sub>3</sub>	0.550 (35)	-25

<sup>a</sup> Numbers *n* in parentheses **2(n)** are for the chain length. <sup>b</sup> Assuming a thermodynamic control of the electron transfers. <sup>c</sup> Two mono-electronic processes.

(dithiafulvenyl) moieties into a bis(cation) radical (reactions 1 and 2 in Scheme 2) and then the coupling to produce a dihydro-dication (reaction 3). The produced dihydro-dication needs to lose two protons to form the final cyclic TTF **2** (reaction 4). As discussed before for the unlinked TTFs, the deprotonation steps that involved C–H acid are slow and occur in the 0.1 s time range.<sup>3b</sup> This explains the low amount of cyclic vinylogous TTF **2** produced on the time scale of the cyclic voltammetry experiment even if the C–C bond is formed at a time lower than  $10^{-4}$  s. The generated TTF is then rapidly oxidized to the corresponding dication at a potential located at the level of the oxidation of **3** (reaction 5). The combination of these two reaction steps is responsible for the crossover visible in Figure 2.<sup>3b,24</sup>

To confirm the nature of the mechanism from the slope value, the knowledge of the difference between the standard potentials ( $\Delta E^\circ = E_2^\circ - E_1^\circ$ , where  $E_1^\circ$  and  $E_2^\circ$  are the individual standard potentials for the oxidation of the two redox centers in the bis-(1,4-dithiafulvenes)) is necessary because the experimental slope value depends on  $\Delta E^\circ$ . In principle, this value can only be extracted from the reversible voltammograms. Unfortunately, the oxidation of **3** remains irreversible even at the largest available scan rates ( $10\,000\text{ V s}^{-1}$ ), indicating that the electro-generated species are highly reactive and that the determination of the standard oxidation potentials (and of  $\Delta E^\circ$ ) is not possible.

However, previous investigations have shown that, for a molecule with two redox centers connected by a nonconjugated chain link of at least four carbons (and longer), the interactions between the two redox centers are weak.<sup>9,25</sup> In such case, the two standard potentials are not exactly the same and differ by  $RT/F \ln 4$  (35.0 mV at 293 K) because there are two possibilities for removing the second electron (entropic factor).<sup>25</sup> We used this value of  $\Delta E^\circ$  in a numerical simulation of the irreversible voltammogram, considering the mechanism depicted in Scheme 2 ( $\Delta E^\circ = 35\text{ mV}$ , fast electron transfers, and fast coupling

(24) See the simulation in the Supporting Information exemplifying this effect.  
(25) Ammar, F.; Savéant, J.-M. *J. Electroanal. Chem.* **1973**, *43*, 115.

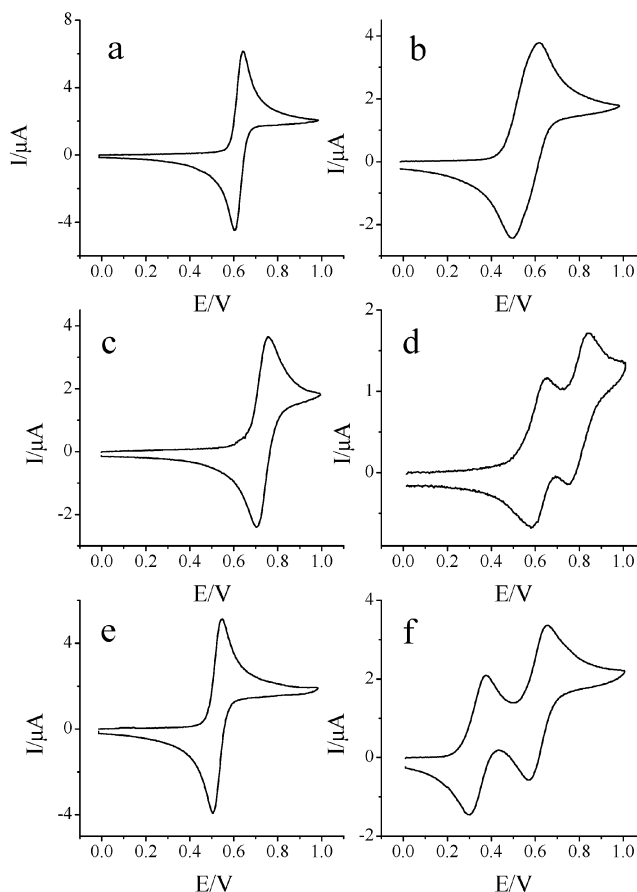


**Figure 2.** Cyclic voltammetry of the TTF vinylogous oxidation on a 1 mm diameter disk gold electrode in  $\text{CH}_2\text{Cl}_2$  +  $0.1\text{ mol L}^{-1}\text{ NBu}_4\text{BF}_4$ . Scan Rate  $0.1\text{ V s}^{-1}$ . (a) **2c(4)** (A = (CH<sub>2</sub>)<sub>4</sub>, R = C<sub>6</sub>H<sub>5</sub>), Conc =  $1.1 \times 10^{-3}\text{ mol L}^{-1}$ . (b) **2c(12)** (A = (CH<sub>2</sub>)<sub>12</sub>, R = C<sub>6</sub>H<sub>5</sub>), Conc =  $1.2 \times 10^{-3}\text{ mol L}^{-1}$ . (c) **2b(4)** (A = (CH<sub>2</sub>)<sub>4</sub>, R = *o*-NCC<sub>6</sub>H<sub>4</sub>), Conc =  $8 \times 10^{-4}\text{ mol L}^{-1}$ . (d) **2b(12)** (A = (CH<sub>2</sub>)<sub>12</sub>, R = *o*-NCC<sub>6</sub>H<sub>4</sub>), Conc =  $1.1 \times 10^{-3}\text{ mol L}^{-1}$ . (e) **2e(4)** (A = (CH<sub>2</sub>)<sub>4</sub>, R = *o*-MeOC<sub>6</sub>H<sub>4</sub>), Conc =  $9 \times 10^{-4}\text{ mol L}^{-1}$ . (f) **2e(12)** (A = (CH<sub>2</sub>)<sub>12</sub>, R = *o*-MeOC<sub>6</sub>H<sub>4</sub>), Conc =  $1.3 \times 10^{-3}\text{ mol L}^{-1}$ . Reference electrode: SCE.

reaction kinetics in the bis(cation) radical), and theoretical variations for the scan rate ( $\partial E_p/\partial \log(v)$ ) of  $15.8\text{ mV}$  and for the initial concentration of **3** ( $\partial E_p/\partial \log(C)$ ) = 0 were predicted for the radical–radical coupling mechanism.<sup>26</sup> The experimental slopes are close to the calculated values for the mechanism involving the coupling in the bis(cation) radical, taking into account that the real experimental  $\Delta E^\circ$  can be slightly larger and thus supports the proposed mechanism in Scheme 2.<sup>27</sup>

(26) (a) A mechanism involving the addition of the radical cation to the other double bond could also be considered. It corresponds to an ECE-DISP<sup>26b–d</sup> mechanism where the chemical step is the addition reaction. In the framework of the ECE-DIPSP mechanism, four possible limiting kinetics situations are encountered: (i) two ECE situations, ECE<sub>rev</sub> and ECE<sub>irr</sub>, where the interference of the homogeneous electron transfer is negligible and where the chemical step is reversible or not and (ii) two DISP situations where the interference of the second heterogeneous electron transfer can be neglected, namely DISP1 and DISP2. In the DISP1 behavior, the rate determining factor is the formation of the C–C bond, while, in the DISP2, the rate determining factor is the homogeneous electron transfer, the coupling reaction acting as a pre-equilibrium. For the first three cases, the predicted slopes are  $(\partial E_p/\partial \log(v)) = 29\text{ mV}$  per decade and  $(\partial E_p/\partial \log(C)) = 0$ . For the DISP2,  $(\partial E_p/\partial \log(v)) = 19.4\text{ mV}$  per decade for the variation with the scan rate and  $(\partial E_p/\partial \log(C)) = -19.4\text{ mV}$  per decade of the concentration.<sup>26b,c</sup> None of these situations correspond to our experimental measurements. (b) Andrieux, C. P.; Nadjo, L.; Savéant, J.-M. *J. Electroanal. Chem.* **1973**, *41*, 137. (c) Andrieux, C. P.; Savéant, J.-M. In *Electrochemical Reactions in Investigation of Rates and Mechanism of Reactions, Techniques of Chemistry*; Bernasconi, C. F., Ed.; Wiley: New York, 1986; Vol. VI/4E, Part 2, pp 305–3910. (d) Bard A. J.; Faulkner L. R. *Electrochemical Methods. Fundamental and Applications 2<sup>nd</sup> edition*. John Wiley & Sons: New York, 2001.

**Redox Behavior of Cyclic Vinylogous TTF.** The redox behaviors of the cyclic derivatives **2** were investigated by cyclic voltammetry in dichloromethane (the cyclic vinylogous TTF have low solubility in acetonitrile). In all cases, the voltammograms were fully reversible even at the lowest available scan rate ( $0.05 \text{ V s}^{-1}$ ), confirming that all the produced species are chemically stable at the time scale of the cyclic voltammetry (lifetimes longer than 30 s). As observed in Figure 2, the oxidation of the neutral TTF to the dication occurs either in two monoelectronic processes or in one bielectronic step, depending on the bridging chain length *A* and on the nature of the substituents *R*. When two monoelectronic steps are observed, the corresponding standard potentials  $E_1^\circ$  and  $E_2^\circ$  are immediately derived as the midpoint between the forward and return scan peaks. When only one bielectronic process is observed, it remains possible to obtain a measure (or estimation) of  $E^\circ$  for the two individual electron transfers.<sup>12</sup> We derived first the formal potential  $E_{2e}^{\circ-}$  for the two-electron process  $E_{2e}^{\circ-} = (E_1^\circ + E_2^\circ)/2$  as the half-sum between the two peak potentials  $E_{2e}^{\circ-} = (E_{pa} + E_{pc})/2$  (where  $E_{pa}$  and  $E_{pc}$  are the anodic and cathodic peak potentials, respectively). If the kinetics of the first and second electron-transfer steps are fast, the potential peak separation  $\Delta E_p = E_{pa} - E_{pc}$  gives an immediate measurement of the difference in standard (formal) potentials  $\Delta E^\circ = E_2^\circ - E_1^\circ$  by comparison with the calculated working curve<sup>28</sup> (and thus the combination of  $E_{2e}^{\circ-}$  and  $\Delta E_p$  gives a measure of  $E_2^\circ$  and  $E_1^\circ$ ).

For an infinite separation ( $E_2^\circ \ll E_1^\circ$ ),  $\Delta E_p$  tends to be 28.25 mV at 20 °C. As quoted before, it means that the determination of the individual potentials becomes very inaccurate (then impossible) for large inversions of potential. Any experimental artifacts such as uncompensated ohmic drop or the influence of the heterogeneous electron-transfer kinetics will tend to increase the  $\Delta E_p$  values and thus the deduced  $\Delta E^\circ$ .<sup>29</sup> For most compounds, we observed that  $\Delta E_p$  reached an almost constant value in the lowest range of scan rates, indicating that both electron-transfer kinetics and associated conformational changes are fast.<sup>29</sup> To minimize all these experimental effects,  $E^\circ$  measurements were always performed at a low scan rate ( $0.1 \text{ V s}^{-1}$ ), and the extracted  $\Delta E^\circ$  values, assuming a thermodynamic control (fast kinetics) of the electron transfers, are gathered in Table 1. However, in the following discussion because of the difficulties to determine the exact kinetics rate constants, it is sufficient to consider the measured  $\Delta E^\circ$  as an upper limit. For the longest bridging chain  $A = (\text{CH}_2)_{12}$ , the redox behavior was found to be strongly dependent both on the donating properties of the phenyl group and on the steric interactions (difference between ortho- and para-substituted phenyl groups in the same family of TTF) as it was previously observed for the noncyclic vinylogous **1**. As seen in Table 1, the bielectronic wave splits into two monoelectronic ones when decreasing the donor strength or passing from the para-substituted to the ortho-substituted phenyl. The similarities between the cyclic TTF **2** with  $A = (\text{CH}_2)_{12}$  and the unlinked ones (**1**) suggest that the bridging chain is too long to restrain the conformational changes and thus does not modify the

electrochemical behavior. On the contrary, when the bis-(thioalkyl) chain is short ( $A = (\text{CH}_2)_4$  or  $(\text{CH}_2)_3$ ), only one reversible wave, associated with concomitant exchange of two electrons, is observed. The neutral TTF is thus directly oxidized to its dicationic form. More precise measurements of the standard potentials show a small decrease of  $\Delta E^\circ$  when increasing the donor properties of the phenyl substituents and very little change with the substituent position.

Variations with the phenyl substituents are slightly higher for  $(\text{CH}_2)_4$  than for the TTF with the  $(\text{CH}_2)_3$  chain and as previously noticed much higher for the  $(\text{CH}_2)_{12}$  chain. Concerning the global oxidation of the neutral TTF to its dication,  $E_{2e}^{\circ-}$ ,<sup>30</sup> we observed that the two-electron redox potential increases when the chain length is slightly decreased for all the substituents *R*, that is,  $E_{2e}^{\circ-}$  (for noncyclic **1a–e**)  $<$   $E_{2e}^{\circ-}$  (for **2a–e(12)**,  $A = (\text{CH}_2)_{12}$ )  $<$   $E_{2e}^{\circ-}$  (for **2a–e(4)**,  $A = (\text{CH}_2)_4$ )  $<$   $E_{2e}^{\circ-}$  (for **2a–e(3)**,  $A = (\text{CH}_2)_3$ ). This general tendency shows a destabilization of the dication and suggests that the molecular movement is considerably modified by the alkyl chain (see later discussion). To investigate the influence of the alkyl chain on the molecular movements, we performed several spectroelectrochemical experiments, where the species produced during exhaustive oxidation are followed by the spectral changes. For the first set of experiments, we chose the series of the *p*-NCC<sub>6</sub>H<sub>4</sub> derivatives **1a**, **2a(12)**, and **2a(3)**. For these three compounds with or without the bis-(thioalkyl) chain, the vinylogous TTF core is oxidized directly into the dication. As a first observation, we notice that similar UV–visible spectra are obtained for all the neutral species (initial spectra before electrolysis in Figure 3), indicating that the presence of the alkyl chain does not considerably modify the conjugation and thus the conformations in the neutral species. Concerning the dications, we observed the spectra evolutions during the oxidation were similar for the unlinked TTF **1a** and the cyclic one **2a(12)**. The dication species produced upon oxidation are clearly visible at  $\lambda_{\text{max}} = 588 \text{ nm}$  for **1a** and  $\lambda_{\text{max}} = 592 \text{ nm}$  for **2a(12)**, indicating the formation of the same conjugated backbone. By contrast, the spectrum of the electrogenerated dication for TTF **2a(3)** exhibits only a broader absorption band at  $\lambda_{\text{max}} = 493 \text{ nm}$ , evidencing a completely different dicationic backbone. For the second set of experiments, we analyzed the *o*-NCC<sub>6</sub>H<sub>4</sub> derivatives where two monoelectronic waves are observed due to steric interactions. This time, the formation of the radical cation (large peak around 600 nm and absorbance in the 710 nm range) was initially visible before the formation of the dication (only one peak around 619 nm) in the case of **1b** and **2b(12)**. On the contrary for the **2b(4)** and **2b(3)** derivatives, the dication is directly produced upon oxidation with a broad absorption band at  $\lambda_{\text{max}} = 520 \text{ nm}$ .

Concerning the effects of the bridge length on the spectra of the neutral and dication, we obtained the same trend with the ortho phenyl derivatives and with the para phenyl substituted compounds. Therefore, we can conclude that the shortest chains,  $(\text{CH}_2)_3$  or  $(\text{CH}_2)_4$ , essentially influence the dications' conformations and that the  $(\text{CH}_2)_{12}$  bridge is still long enough to enable a stretch movement as observed in the nonlinked molecules.

**Molecular Modeling and X-ray Investigations.** Based on molecular modelings and experimental results from X-ray crystallographic structures, we previously found for the unlinked

(27) As expected, a larger  $\Delta E^\circ$  induced an increase of  $(\partial E_p/\partial \log(v))$ . This point was checked with numerical simulations (Digisim 3.1).

(28) (a) Myers, R. L.; Shain, I. *Anal. Chem.* **1969**, *41*, 980. (b) Andrieux, C. P.; Savéant, J.-M. *J. Electroanal. Chem.* **1974**, *57*, 27.

(29) Evans, D. H. *Acta Chem. Scand.* **1998**, *52*, 194.

(30) For reversible redox systems, the half sum potential  $E_{1/2}$  is equal to the bielectronic formal potential  $E_{2e}^{\circ-}$ .

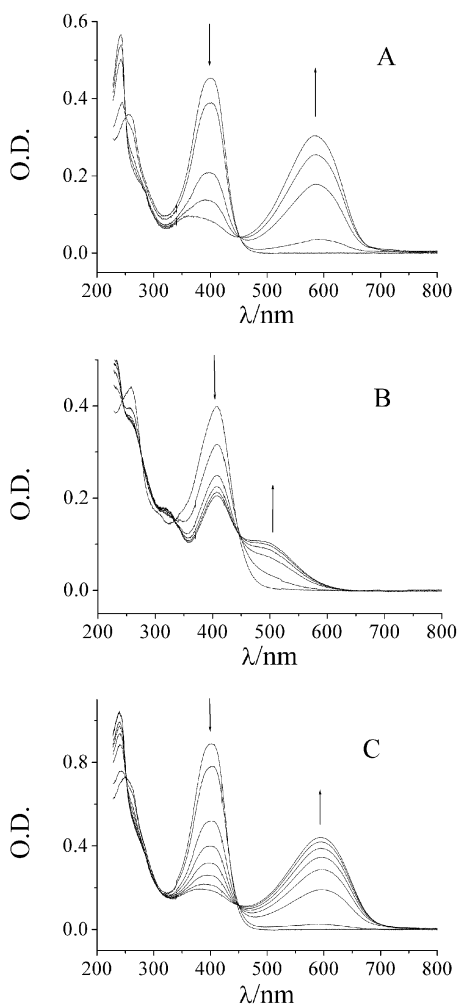


**Figure 3.** UV-visible spectroelectrochemistry of *p*-NCC<sub>6</sub>H<sub>4</sub> derivatives in CH<sub>2</sub>Cl<sub>2</sub> (+ 0.1 mol L<sup>-1</sup>). Oxidation on a platinum grid inserted in a 1 mm quartz cell. (A)  $1.2 \times 10^{-4}$  mol L<sup>-1</sup> **1a**, (B)  $1.2 \times 10^{-4}$  mol L<sup>-1</sup> **2a(3)**, and (C)  $2.5 \times 10^{-4}$  mol L<sup>-1</sup> **2a(12)**. (↓) Initial spectrum. (↑) During oxidation (the 400 nm band decreases as the 500–600 nm band increases). Oxidation potential: 1.0 V/SCE.

vinyllogous TTF **1** that the inversion (or compression) of potentials is related to large conformational modifications associated with a fast electron transfer.

The values derived for the linked TTF **2** show that “potential inversions” exist for both families of TTF. However, the differences of  $\Delta E^\circ$  between **1** and **2**, especially for the shortest bridging chains, confirm that an additional steric hindrance exists in the linked TTF. Considering that the inversions of potentials for **2** are demonstrative of the existence of conformational changes as for the noncyclic analogue, we find the remaining question for the cyclic molecules concerns the nature of the possible structural changes associated with the electron transfer. To answer to this question, we investigated the molecular structure of the neutral donors **2b(4)**, **2a(4)**,<sup>9</sup> and **2a(3)** by single-crystal X-ray analysis. We obtained the dicationic salts of **2d(4)** by exposing a solution of the donor in CH<sub>2</sub>Cl<sub>2</sub> to an iodine atmosphere. For TTF **1**, the neutral donors are nonplanar while in the oxidized states (cation radical or dication) the donor cores adopt a planar geometry with the bulky substituents located in perpendicular planes.<sup>3a,11a–b,12</sup> For the neutral form of the cyclic TTF **2**, experiments reveal a nonplanar geometry similar to their noncyclic analogues (see Figure 4). The influence of the ortho/

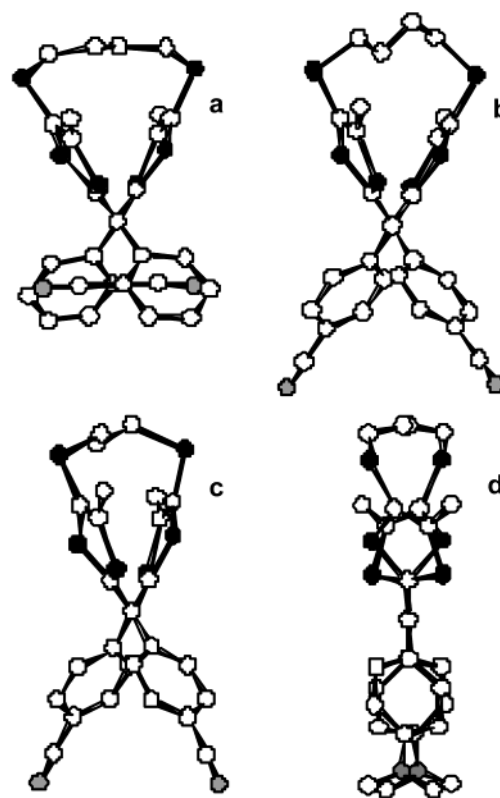


**Figure 4.** Crystallographic molecular structures of neutral. (a) **2b(4)** (R = *o*-NCC<sub>6</sub>H<sub>4</sub>, A = (CH<sub>2</sub>)<sub>4</sub>), (b) **2a(4)** (R = *p*-NCC<sub>6</sub>H<sub>4</sub>, A = (CH<sub>2</sub>)<sub>4</sub>), (c) **2a(3)** (R = *p*-NCC<sub>6</sub>H<sub>4</sub>, A = (CH<sub>2</sub>)<sub>3</sub>), and (d) dication of **2d(4)** (R = *p*-MeOC<sub>6</sub>H<sub>4</sub>, A = (CH<sub>2</sub>)<sub>4</sub>) viewed along the central C–C axis (sulfur atoms in black, nitrogen and oxygen atoms in gray).

para substituent position and the chain length can be seen in Figure 4 where the molecules **2b(4)**, **2a(4)**, and **2a(3)** are viewed along the central C–C axis. As expected, the molecular geometry is more constrained with the shortest (CH<sub>2</sub>)<sub>3</sub> link. The two acute dihedral angles based on this central C–C bond in **2b(4)** amount to 69.0(2)° and 69.2(2)° for the two dithiole rings and the two phenyl rings, respectively. These angles decrease to 65.2(6)° and 62.4(6)° for the para-substituted one **2a(4)** and to 60.4(6)° and 57.8(6)° for the shortest link in **2a(3)**. Under its dicationic form, the donor core of **2** adopts a new conformation largely different to the one observed for the unlinked TTF **1** (see Figure 4d).<sup>11</sup> Indeed, the values for the two acute dihedral angles for the dication **2d(4)**<sup>2+</sup> are now 3(1)° and 0(1)°. To obtain additional information on the other molecules and on the radical cationic state, we used molecular modeling calculations to determine both the geometries and the stabilities of the TTF in their three oxidation states. These calculations provide useful information on the molecular geometries when data are not available from the X-ray experiments and for all the redox states. As we previously reported for the unlinked TTF, molecular modeling based on DFT (density functional theory) gives a good agreement between X-ray data and calculated conformations for the linked TTF and can be used to predict the evolution of the TTF properties with the substituent.<sup>12</sup> For the bridged neutral TTF, the chain link does not affect considerably the geometry and the energy of the donors (Figure 5a and c) because of the single character of the central C–C bond. On the contrary, for the dicationic form, the (C<sub>3</sub> and C<sub>4</sub>) chains are clearly too short for allowing the vinyllogous TTF core to reach its planarity (Figure 5b and d). This observation



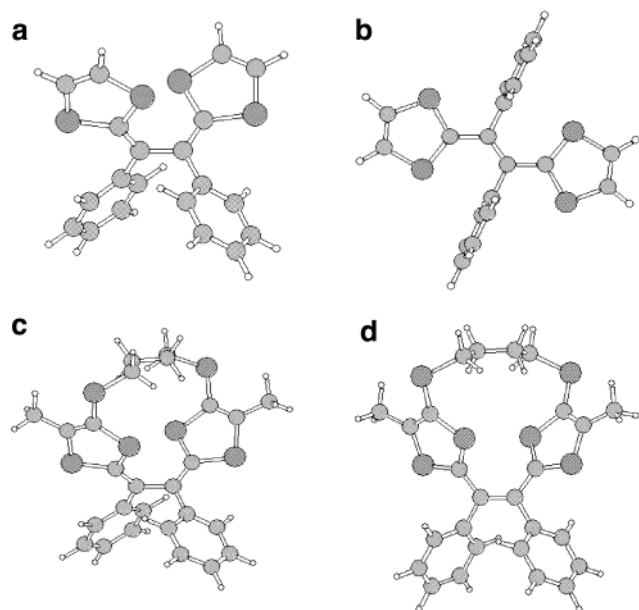


**Figure 5.** Comparison of conformation changes between vinylogous TTF and their cyclic analogues. Optimized geometries calculated at the B3LYP/6-31G\* level of the neutral (a, c) and dication (b, d) of **1c** (a, b) and **2c(4)** (c, d) (R = C<sub>6</sub>H<sub>5</sub>, A = (CH<sub>2</sub>)<sub>4</sub>).

explains the experimental results (see previous text); the dication is more destabilized by the presence of the alkyl chain link than the neutral TTF, inducing bielectronic oxidation potentials  $E_{2e}^{\circ}$  more positive for the cyclic TTF than for the unlinked compounds. This effect increases when the chain link becomes shorter.

Concerning the molecular movement, we observe the bis-(thioalkyl) link restrains the conformation modifications upon oxidation as compared to the noncyclic analogues, resulting in different conformational changes. The molecule now acts as a type of molecular clip that can be closed with the electronic transfer (see Figure 6). Because the induced movements are different, the influence of the substituents on the conformers' energies (and thus on the variation of  $\Delta E^{\circ}$  with the substituents) has no reason to be similar for cyclic and noncyclic TTF. As we can derive from the  $\Delta E^{\circ}$  variations in Table 1, the position of the substituent on the phenyl ring (ortho or para) strongly affects the conformational changes in the noncyclic TTF and has little interference on the conformational changes in the case of the cyclic TTF.

A more quantitative description can be obtained from the variations of the disproportionation free energies. They reflect the radical cation stability and take into account the structural changes associated with all the redox states.

$$2 \text{TTF}^{\bullet+} \rightleftharpoons \text{TTF}^{2+} + \text{TTF}, \Delta G_{\text{disp}}^{\circ}, K = \exp\{(E_1^{\circ} - E_2^{\circ})F/RT\}$$

A first approach is to compare the experimental data  $\Delta G_{\text{disp}}^{\circ}$  ( $\Delta E^{\circ}$ ) with the variation of the electronic energies for the disproportionation reaction  $\Delta U_{\text{el,disp}}$  calculated by DFT in gas phase (where  $\Delta U_{\text{el,disp}}$  are the differences between the electronic energies in gas phase; Table 2). However, a large part of the free energy in gas phase has an electrostatic origin, and it is necessary to estimate the solvation free energies  $\Delta G_{\text{solv}}^{\circ}$  for a comparison with the experimental variations of  $\Delta G_{\text{disp}}^{\circ}$ . As we

have done previously for the noncyclic TTF, we used the IPCM method where the solvent is described as a dielectric continuum and the conformations are those previously optimized in the gas-phase calculations.<sup>31</sup> Thus,  $\Delta U_{\text{el,disp}} + \Delta G_{\text{solv,disp}}^{\circ} = U_{\text{el}}(\text{dication}) + U_{\text{el}}(\text{neutral}) - 2U_{\text{el}}(\text{radical cation}) + \Delta G_{\text{solv}}^{\circ}(\text{dication}) + \Delta G_{\text{solv}}^{\circ}(\text{neutral}) - 2\Delta G_{\text{solv}}^{\circ}(\text{radical cation})$ .<sup>32</sup> As often obtained in such comparisons, the estimated values are higher than the experimentally observed  $\Delta G_{\text{disp}}^{\circ}$ , but the relative variations provide a good description of the experimental trends.<sup>12</sup>

For the longest chain (A = (CH<sub>2</sub>)<sub>12</sub>), the  $\Delta U_{\text{el,disp}}$  in gas-phase values display similar variations than the ones observed for the noncyclic TTF.<sup>33</sup> It confirms the experimental observation that the constraints introduced by the C<sub>12</sub> chain are quite weak and that the length of the chain is long enough to let the dication to be almost planar. For the cyclic TTF **2** with the shortest chain links (A = (CH<sub>2</sub>)<sub>4</sub>, (CH<sub>2</sub>)<sub>3</sub>), the calculated  $\Delta U_{\text{el,disp}} + \Delta G_{\text{solv,disp}}^{\circ}$  display very little change with the substituent on the phenyl group in good agreement with the experimental values on the opposite of the noncyclic **1** where both experimental and DFT estimations show considerable changes in  $\Delta G_{\text{disp}}^{\circ}$ . When passing from a donor to a withdrawing substituent,  $E_{2e}^{\circ}$  becomes more positive as expected from a decrease of the donor character, but the variations on the individual standard potentials for the first and second oxidation states ( $E_1^{\circ}$  and  $E_2^{\circ}$ ) are very similar ( $\Delta E^{\circ}$  almost constant). Calculations and experiments show (i) that the substituent effect on the donor properties are not modified by the conformational changes and (ii) that we do not have an extra stabilization (or destabilization) of one redox state versus another one due to the substituent R. Similarly, we do not observe a considerable difference in  $\Delta E^{\circ}$  between the ortho- and para-substituted TTF **3** because the twisted configurations for both the neutral and dication (see Figures 2–4) induce a similar steric hindrance with the ortho substituent. This is an interesting behavior for molecular engineering, because, when adding another chemical group on the molecular clamp (for example to design a chemical trap), we can expect that the conformational changes will not kill the designed properties.

Concerning the calculated geometries, we summarized in Table 3, the variations of the bond lengths and dihedral angles between the two phenyl rings for **1c**, **2c(3)**, and **2c(4)**. As expected, the main modifications with the redox state are located on the vinylogous system of the TTF core, the lengths of the central C–C bond (a) and the C–S bonds (c) are shortened while the other bonds C–C (b) are increased, and similar variations are visible for all the TTF. The radical cation conformation is almost in the middle between neutral and the dication conformations. On the contrary, for the noncyclic TTF **1**, we found that most of the changes occur after the first oxidation (the radical cation has a planar conformation similar to the dicationic state). This is illustrated in Table 3 by the

- (31) Conformations of charged species in the presence of a solvent can be slightly modified from the optimization made in gas phase. This approach was chosen as a compromise between calculation time and precision because optimizations in the presence of solvent would have required unrealistic calculations times.
- (32) As previously found,<sup>12</sup> for a comparison inside the same family of TTF molecules, the differences of thermal and ZPE corrections among the neutral, radical cation, and dication corresponding to the disproportionation reactions are small and can be negligible for the analysis of the general trend.
- (33) Calculations of  $\Delta G_{\text{solv,disp}}^{\circ}$  were not possible for the C<sub>12</sub> compounds because of the too large molecule size.

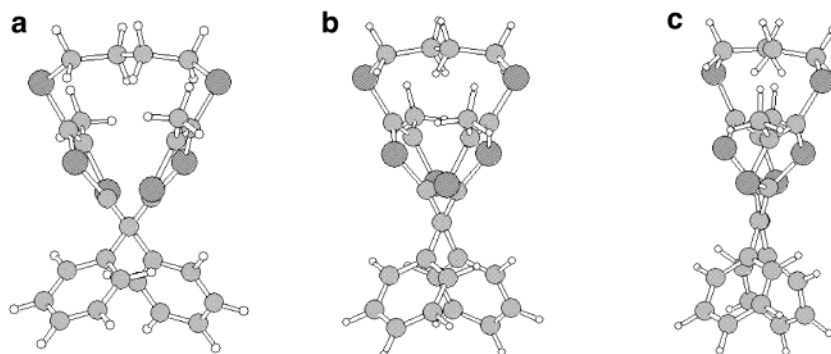
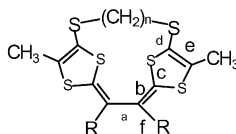


**Figure 6.** Optimized geometries calculated at the B3LYP/6-31G\* level of the neutral (a), radical cation (b), and dication (c) of **2c(4)** (R = C<sub>6</sub>H<sub>5</sub>, A = (CH<sub>2</sub>)<sub>4</sub>).

**Table 2.** Calculated  $\Delta U_{\text{el,Disp}}$  and Comparison with Experimental  $\Delta E^\circ$  for Cyclic vinylogous TTF **3**

compound	R	A	$\Delta U_{\text{el,disp}}$ in a vacuum in V	$\Delta U_{\text{el,disp}} + \Delta G_{\text{sol,disp}}^\circ$ in CH <sub>2</sub> Cl <sub>2</sub> in V	$\Delta E^\circ/V$ in CH <sub>2</sub> Cl <sub>2</sub> in V exptl
<b>1a</b>	<i>p</i> -NCC <sub>6</sub> H <sub>4</sub>		3.42	0.72	−25
<b>1c</b>	C <sub>6</sub> H <sub>5</sub>		3.58	0.81	76
<b>1d</b>	<i>p</i> -MeOC <sub>6</sub> H <sub>4</sub>		3.45	0.88	104
<b>2a(12)</b>	<i>p</i> -NCC <sub>6</sub> H <sub>4</sub>	(CH <sub>2</sub> ) <sub>12</sub>	2.96		36
<b>2c(12)</b>	C <sub>6</sub> H <sub>5</sub>	(CH <sub>2</sub> ) <sub>12</sub>	3.11		85
<b>2a(4)</b>	<i>p</i> -NCC <sub>6</sub> H <sub>4</sub>	(CH <sub>2</sub> ) <sub>4</sub>	3.03	0.65	−13
<b>2c(4)</b>	C <sub>6</sub> H <sub>5</sub>	(CH <sub>2</sub> ) <sub>4</sub>	3.15	0.68	−25
<b>2d(4)</b>	<i>p</i> -MeOC <sub>6</sub> H <sub>4</sub>	(CH <sub>2</sub> ) <sub>4</sub>	3.05	0.71	−13
<b>2a(3)</b>	<i>p</i> -NCC <sub>6</sub> H <sub>4</sub>	(CH <sub>2</sub> ) <sub>3</sub>	3.06	0.67	−3
<b>2c(3)</b>	C <sub>6</sub> H <sub>5</sub>	(CH <sub>2</sub> ) <sub>3</sub>	3.19	0.68	−7
<b>2d(3)</b>	<i>p</i> -MeOC <sub>6</sub> H <sub>4</sub>	(CH <sub>2</sub> ) <sub>3</sub>	3.05	0.67	−13

**Table 3.** B3LYP/6-31G\* Optimized Geometries: Bond Lengths (Å) and Dihedral Angles (deg) of Cyclic Vinylogous TTF (Neutral, Radical Cation, Dication)



compound	R	A	a	b	c	d	e	f	dihedral angles	
									(bab)	(faf)
<b>1c<sup>a</sup></b>	C <sub>6</sub> H <sub>5</sub>		1.501	1.361	1.792	1.761	1.337	1.489	73.6	69.5
			1.422	1.412	1.758	1.739	1.345	1.502	178.6	176.6
			1.384	1.458	1.723	1.727	1.358	1.499	180.0	180.0
<b>2c(3)</b>	C <sub>6</sub> H <sub>5</sub>	(CH <sub>2</sub> ) <sub>3</sub>	1.503	1.362	1.779	1.782	1.350	1.485	69.7	67.6
			1.461	1.399	1.748	1.771	1.361	1.482	46.7	43.9
			1.411	1.452	1.713	1.758	1.372	1.480	22.4	23.5
<b>2c(4)</b>	C <sub>6</sub> H <sub>5</sub>	(CH <sub>2</sub> ) <sub>4</sub>	1.504	1.362	1.781	1.784	1.349	1.486	75.2	71.2
			1.461	1.397	1.750	1.772	1.362	1.486	51.3	46.3
			1.411	1.450	1.719	1.761	1.377	1.484	26.5	24.9

<sup>a</sup> from ref 12.

variation of the dihedral angle (that describes the amplitude of the cage closing with the electron transfer in the case of **2**).

For unlinked TTF **1**, the angles for the radical cation are the same as those for the dication. For the cyclic **2**, this is obviously not the case; dihedral angles are almost in the midpoint between the values for the neutral and the dication, showing that the conformational changes occur after the first and the second electron transfers. For the cyclic TTF **3**, it is also visible that angles and distances are only slightly affected by the nature of the substituent on the phenyl group, supporting the previous discussion. According to the calculations, if we want to maximize the amplitude of the molecular movements of the clamp, it is better to use a phenyl with a withdrawing group

and a chain around four carbons. To finish the comparison between theoretical expectations and experimental X-ray investigations, detailed examinations of the results indicate that the closing of the clamp is higher in the crystal than predicted by the calculations. If we cannot reject some difficulties due to the DFT method in the energies calculations and in the optimization process, we should take into account a possible packing effect in the crystal that will be lower or inexistent in the gas phase or for a molecule in dilute solution.

## Conclusion

The use of a link connecting the dithiole rings through the outer sulfur atoms of the vinylogous TTF core modifies



marginally the donor ability of these molecules. Interestingly, this additional steric strain induces an opposite conformational change upon oxidation to the stretch one observed for the unlinked vinylogous TTFs. Indeed, these cyclic vinylogous TTFs, with a short bis(thioalkyl) link, act as a fast and reversible molecular clip that can be closed by electron transfer. The movement appears to be almost insensitive to the nature of the substituents or its steric hindrance on the central conjugated spacer between the dithiole rings. For instance, the phenyl rings remain in a twisted position in all the redox states and therefore do not interfere in the closing of the molecular clamp. We have developed an easy route, with regard of the quantity (gram scale) and the simplicity of the synthesis, to novel molecular clips triggered by electron transfer. Various substituents, other than phenyl groups, can be envisaged on the central conjugation according to the chemical pathway used to reach these cyclic vinylogous TTFs. For future uses of this system in molecular engineering, this is an advantage, as the introduction of

functional substituent, to prepare a trap or a sensor, should not change the nature of the molecular movement.

**Acknowledgment.** The authors are indebted to Dr J.-F. Bergamini for his help in the spectroelectrochemical experiments.

**Supporting Information Available:** Voltammogram simulation and parameters of **3b(4)** oxidation (Table and Figure) with Digisim 3.1. Experimental oxidation peak potentials of bis(1,4-dithiafulvenes) **3(n)** in CH<sub>2</sub>Cl<sub>2</sub> (Table). X-ray crystallographic data for structure determination of **2a(4)**, **2b(4)**, **2a(3)**, and **2d(4)<sup>2+</sup>** (CIF)(Table). B3LYP/6-31G\*energies in gas phase and CH<sub>2</sub>Cl<sub>2</sub> for **2a(3)**, **2c(3)**, **2d(3)**, **2a(4)**, **2c(4)**, **2d(4)**, **2a(12)**, and **2c(12)** (Table). This material is available free of charge via the Internet at <http://pubs.acs.org>.

JA0289090